Multiplex immunohistochemistry elucidates increased distance between cytotoxic T cells and plasma cells in relapsed myeloma, and identifies Lag-3 as the most common checkpoint receptor on cytotoxic T cells of myeloma patients

Slavisa Ninkovic,[1,2,3] Louise E Purton,[2,3] Simon J Harrison[4,5] and Hang Quach[1,2]

[1]Department of Haematology, St. Vincent's Hospital Melbourne, Melbourne; [2]Faculty of Medicine, University of Melbourne, St. Vincent's Hospital, Melbourne; [3]Stem Cell Regulation Unit, St. Vincent's Institute of Medical Research, Melbourne; [4]Clinical Haematology, Peter MacCallum Cancer Centre and The Royal Melbourne Hospital, Melbourne and [5]Sir Peter MacCallum Department of Oncology, University of Melbourne, Parkville, Victoria, Australia

Correspondence: S. Ninkovic
slavisa.ninkovic@svha.org.au

Received: May 18, 2023.
Accepted: October 12, 2023.
Early view: October 19, 2023.

https://doi.org/10.3324/haematol.2023.283344

Abstract

A dysfunctional immune tumor microenvironment facilitates disease progression in multiple myeloma (MM). Using multiplex immunohistochemistry (mIHC), we describe the quantitative and qualitative changes in $CD3^+CD8^+$ cytotoxic T cells and assess their proximity to malignant plasma cells (PC) in patients with monoclonal gammopathy of undetermined significance (MGUS), and newly diagnosed (ND) and relapsed and/or refractory (RR) MM. Formalin-fixed, paraffin-embedded trephine sections from patients with MGUS (N=32), NDMM (N=65), and RRMM (N=59) were sequentially stained for CD138, CD3, CD8, and checkpoint receptors (CPR) Tim-3, Lag-3, and PD-1. The Halo® image analysis platform was used for cell segmentation and phenotyping, facilitating enumeration of cytotoxic T cells and analysis of proximity to PC. The percentage of $CD8^+$ cytotoxic T cells in proximity to PC is greater in patients with NDMM than patients with RRMM (at 50 μm distance, 90.8% *vs.* 81.5%; *P*=0.038). There is a trend for more $CD3^+$ T cells in MGUS (*P*=0.08) but no difference was observed in the prevalence of $CD8^+$ cytotoxic T cells (*P*=0.48). Lag-3 is the most common CPR expressed on cytotoxic T cells in myeloma (*P*<0.0001), while PD-1 is the most common CPR on $CD8^-$ T cells of patients with MGUS and RRMM. Our study is the first to report on the spatial relationship between T cells and PC using mIHC on FFPE bone marrow trephine sections from patients with PC dyscrasia. The proximity of T cells to PC during early stages of MM, and overexpression of Lag-3, validate the move of immune therapeutic strategies, including T-cell engagers and checkpoint inhibitors, to upfront treatment or in early-line treatment of MM.

Introduction

Multiple myeloma (MM) is an incurable malignancy, preceded by the precursor condition monoclonal gammopathy of undetermined significance (MGUS). Despite recent advances in treatment strategies, MM is characterized by recurrent relapses with progressively shorter duration of response and treatment-free intervals. Dysregulation and dysfunction of the immune tumor microenvironment (iTME) is one of the key pillars in myeloma pathogenesis and progression, with many recently approved anti-myeloma therapies specifically targeting the immune system.[1-3]

Qualitative and quantitative alterations of the T-cell repertoire contributing to disease progression are in part characterized by an early increase in cytotoxic $CD3^+CD8^+$ T cells.[4] Cytotoxic T cells isolated from patients with MGUS exert vigorous anti-tumor-specific responses to autologous myeloma cells, but overstimulation and chronic tumor-associated antigen exposure leads to T-cell exhaustion.[5-7] Exhaustion is, in part, characterized by expression of inhibitory check-

point receptors including programmed death receptor-1 (PD-1), T-cell immunoglobulin 3 (Tim-3), lymphocyte activation gene-3 (Lag-3), and T-cell immunoglobulin and ITIM domains (TIGIT).[8-11] Recent studies exploring the immune dysfunction as a contributing factor to disease relapse have consistently shown an association between higher levels of PD-1, Tim-3, Lag-3 or TIGIT and disease outcomes.[9,11-15] Therapeutic targeting of inhibitory checkpoint receptors with monoclonal antibodies is in various stages of pre-clinical and clinical development, with targeting of the PD-1/PD-L1 axis being examined most extensively. The combination of pembrolizumab, an anti-PD-1 monoclonal antibody (mAb), with standard-of-care anti-myeloma immunomodulatory (IMiD) drugs lenalidomide or pomalidomide, achieved a 44% or 60% overall response rate (ORR) in relapsed/refractory (RR) patients. However, patients treated with this novel combination had a shorter progression-free survival (PFS) and higher treatment-related deaths, resulting in the suspension of clinical trials of the anti-PD-1 and IMiD combination.[16-18] An alternative approach to re-invigorate the iTME is to bring cytotoxic T cells and plasma cells (PC) into physical proximity with the use of bispecific mAb. These so-called T-cell engagers are capable of binding two different antigens: one specific to T cells and the other a tumor-associated antigen present on malignant PC.[3] Previous studies have demonstrated a link between T-cell and malignant cell proximity with response to immunotherapy in patients with solid tumors like melanoma, yet little is known about the spatial relationship between cytotoxic T cells and PC in myeloma.[19-21] Recent studies, often using flow cytometry, mass cytometry by time-of-flight (CyTOF) or single cell RNA sequencing (scRNA-seq), have enriched our understanding of iTME characteristics in patients with myeloma and precursor conditions.[22-24] While scRNA-seq and CyTOF can be very informative, they depend on the assessment of individual cells isolated from the bone marrow aspirate (BMA), making it impossible to comment on the BM architecture or the spatial relationships between PC and various components of the iTME. Using multiplex immuno-fluorescence histochemistry (mIHC), a technique that preserves BM architecture while allowing the simultaneous detection of up to six antigens, we aimed to improve our understanding and describe the iTME in the trephine of patients with MGUS, and ND and RR MM. Specifically, we focused on cytotoxic T cells as defined by cell membrane co-expression of CD3 and CD8 and the expression pattern of inhibitory checkpoint receptors, Tim-3, Lag-3, and PD-1. In addition, we set out to describe the spatial relationship between cytotoxic T cells and malignant PC in these three patient cohorts.

Methods

Patient selection

Patients with a diagnosis of MGUS or MM were identified following review of the St. Vincent's Hospital Melbourne (SVHM) BM pathology database from January 2016 to September 2019 inclusive. Diagnostic biopsies were performed as part of standard work-up of suspected PC dyscrasia, while patients in the RR cohort had biopsies performed prior to any subsequent anti-myeloma therapy. Stored formalin-fixed, paraffin-embedded (FFPE) BM trephine (BMT) blocks were retrieved for use in this study, and up to ten 3μm-thick consecutive sections were obtained from patients with MGUS (N=32), NDMM (N=65), and RRMM (N=59). Retrospective data including patient demographics, diagnostic BMA, and BMT PC burden, MM disease characteristics, prior treatment, and response history and survival were extracted from institutional medical records. This study was approved by the SVHM Human Research Ethics Committee in accordance with National Health and Medical Research Council Act 1992 and the National Statement on Ethical Conduct in Human Research 2007 (updated July 2018; approval number LRR 081/19).

Multiplex immunohistochemistry Opal™ workflow, image acquisition, and data analysis

Formalin-fixed, paraffin-embedded sections were subject to deparaffinization and rehydration by serial passage through changes of xylene and graded ethanol followed by heat-induced epitope retrieval (HIER) using a Leica Bond Max Autostainer (Leica Biosystems). Slides were incubated with an anti-human primary antibody, in order of staining: rabbit monoclonal anti-Lag-3 (D2G40/1:400/Cell Signalling Technology, CST), mouse monoclonal anti-CD8 (C8-144B/1:400/CST), rabbit monoclonal anti-CD3 (CD3 epsilon/1:400/CST), rabbit monoclonal anti-PD-1 (D4W2J/1:200/CST), mouse monoclonal anti-CD138 (1:800/Dako Cell Signalling), and rabbit monoclonal anti-Tim-3 (D5D5R/1:400/CST). This was followed by an endogenous tissue peroxidase block with 0.3% hydrogen peroxide and subsequent application of polymeric HRP-conjugated secondary antibody (Leica Biosystems). The immunofluorescent signal was facilitated by application of the Opal™ 7-color fluorescent IHC kit (Akoya Biosciences) with application of the fluorophore-conjugated Tyramide Signal Amplification (TSA; Akoya Biosciences) at a 1:100 dilution (in order of staining: 650, 570, 690, 620, 520, 540). Following Opal-TSA signal deposition, slides were again subjected to HIER, resulting in stripping of tissue-bound primary/secondary antibody complexes with preservation of the tyrosine-residue bound Opal-TSA signal. This process was repeated until all six markers of interest were labeled, followed by a nuclear DAPI counterstain.

Digital, fluorescent images were acquired using the Vectra® 3.0 Automated Quantitative Pathology Imaging System (Akoya Biosciences). Using a set of positive control library slides for each Opal fluorophore, acquired images were spectrally unmixed with inForm® Tissue Analysis Software (v2.4.8; Akoya Biosciences). Halo® Image Analysis Platform (v3.2.1; Indica Labs®) was used for all subsequent stages

of image analysis. Machine-learned tissue segmentation into BM and fat spaces was followed by cell segmentation using nuclear DAPI staining. Detection of a cell membrane (CM) primary antibody signal, in addition to DAPI nuclear staining, allowed for cell phenotyping. Thresholds for positive detection of signals were reviewed in at least five x40 magnification fields for each marker individually for all imaged slides. Cells expressing CM CD138 were identified as PC; all others were classed as non-PC. Expression of CD3 (lymphocytes), CD3 and CD8 (cytotoxic T cells), and checkpoint receptors (TIM-3, LAG-3 or PD-1) allowed for identification of various subsets of T lymphocytes (e.g., Tim-3, CD3, and CD8 co-localization was representative of a cytotoxic T cell expressing the checkpoint receptor Tim-3). An algorithm that considers the percentage of positively stained cells and the fluorescence intensity (low, medium, and high) was applied resulting in an H-score, i.e., a semi-quantitative measure of biomarker intensity. Proximity and nearest neighbor analysis were used to assess the spatial relationship between immune and plasma cells.

Survival definitions and statistical analysis

Overall survival (OS) and PFS were defined as the time from diagnosis (MGUS patients) or initial treatment (ND and RR patients) until death from any cause for OS and disease progression or death from any cause for PFS. Descriptive statistics are presented where appropriate. Normal distribution of data was assessed with the Anderson-Darling test with subsequent application of unpaired *t* test or Mann-Whitney test, as appropriate, for comparisons between two groups. Differences between the three cohorts were analyzed with the ordinary one-way ANOVA or Kruskal-Wallis test as appropriate. All comparisons and all comparative tests were two-tailed with probability values below 0.05 considered statistically significant. Survival rates were estimated using the Kaplan-Meier method. All statistical analyses were performed using GraphPad Prism (v9.2.0 for macOS; GraphPad Software).

Results

Patients' characteristics and treatment outcomes

Patients' and key disease characteristics are shown in Table 1. Treatment and outcomes in the NDMM and RRMM cohorts are shown in Table 2. Applying the MGUS risk stratification model which considers serum monoclonal protein (MP) level and subtype along with presence of abnormal serum free light chain (SFLC) ratio, patients were stratified into low (N=7), intermediate-low (N=14), intermediate-high (N=10), and high (N=1) risk for progression to MM.[25] At a median follow-up time of 2.07±1.26 years post-BM biopsy, 5 patients had progressed to myeloma and 2 had died.

Of the 65 ND patients, 6 had smouldering MM not requiring immediate treatment. First-line therapy was heterogeneous with various combinations of proteosome inhibitor (PI),

Table 1. Patients' and disease characteristics in patients with monoclonal gammopathy of undetermined significance, newly diagnosed multiple myeloma, and relapsed and/or refractory multiple myeloma.

Characteristics	MGUS	NDMM	RRMM	*P*
N of patients	32	65	59	
Median age at time of BMBx in years (range)	74.2 (26.6-87.8)	69.3 (30.5-89.8)	68.8 (34.0-86.2)	0.8025
Gender, N Male Female	 16 16	 40 25	 39 20	0.3201
M-protein subtype, N IgA IgG IgM or IgD None	 6 22 1 3	 10 46 0 9	 6 32 1 20	0.0443
M-protein level, g/L, mean ± SD	11.0±9.0	32.2±20.6	27.5±30.1	<0.0001* 1 *vs.* 2 < 0.0001 1 *vs.* 3 < 0.0006 2 *vs.* 3 = 0.4000
Involved – uninvolved SFLC difference, mean ± SD	286±361	1,193±1,879	998±1,755	0.0301* 1 *vs.* 2 = 0.0253 1 *vs.* 3 = 0.0990 2 *vs.* 3 > 0.9999

BMBx: bone marrow biopsy; M-protein: monoclonal protein; MGUS: monoclonal gammopathy of undetermined significance; NDMM: newly diagnosed multiple myeloma; RRMM: relapsed and/or refractory multiple myeloma; SD: standard deviation; SFLC: serum free light chain. *Ordinary one-way ANOVA or Kruskal-Wallis tests as appropriate with corresponding Tukey's or Dunn's multiple comparisons tests where significance was detected between groups and where: 1 = MGUS, 2 = NDMM, and 3 = RRMM cohort.

Table 2. Treatment and outcomes of newly diagnosed and relapsed and/or refractory multiple myeloma patients.

	NDMM, N=65	RRMM, N=59
Treatment, N (%)		
PI	31 (47.6)	8 (13.6)
IMiD	16 (24.6)	4 (6.8)
PI + IMiD	6 (9.2)	5 (8.5)
PI + mAb	2 (3.1)	18 (30.5)
IMiD + mAb	1 (1.5)	3 (5.1)
PI + IMiD + mAb	3 (4.6)	0
mAb	0	3 (5.1)
Anti-BCMA ADC + IMiD	0	1 (1.7)
Anti-BCMA ADC + PI	0	7 (11.9)
Anti-BCMA BITE	0	6 (10.2)
No treatment	6 (9.2)	4 (6.8)
Best response to therapy, N (%)		
MR/SD	6 (10.2)	7 (11.9)
PR	18 (30.5)	15 (25.4)
VGPR	20 (33.9)	9 (15.3)
CR	9 (15.3)	12 (20.3)
PD	6 (10.2)	16 (27.2)

NDMM: newly diagnosed multiple myeloma; RRMM: relapsed and/or refractory multiple myeloma; PI: proteasome inhibitor; IMiD: immunomodulatory drug; mAb: monoclonal antibody; BCMA: B-cell maturation antigen; ADC: antibody drug conjugate; BITE: bispecific T-cell engager; MR: minor response; SD: stable disease; PR: partial response; VGPR: very good partial response; CR: complete response; PD: progressive disease.

ImiD, and/or anti-CD38 mAb delivered (Table 2). Thirty-one patients (47.7%) had an upfront autologous stem cell transplant (autoSCT). ORR was 79.7%, while 6 patients (10.2%) had stable disease (SD) or a minor response (MR) as their best response to first-line therapy. Six patients progressed while on first-line therapy. At a median follow-up of 2.28±1.08 years, 32 patients had progressed for a median PFS of 2.25 years, while 9 patients had died; the median OS was not reached.

Median time between MM diagnosis and BM biopsy (BM-Bx) utilized for mIHC assessment in the RR cohort was 4.94±3.25 years. A median of 2 (range 1-9) prior lines of therapy were given, with 89.9% of the cohort previously exposed to PI and 54.2% exposed to IMiD. Thirty-four patients (57.6%) had had a previous autoSCT. Treatment was heterogeneous with nine different regimens used (Table 2). Four patients did not receive treatment: 3 due to poor performance status, one due to patient preference. The ORR was 61% with suboptimal response (SD or MR) in 11.9% of patients while 27.2% progressed during therapy. At a median follow-up of 2.43 years, 45 patients had experienced disease progression for a median PFS of 1.08 years, while 23 patients had died, for a 5-year OS of just over 50%.

Multiplex immunohistochemistry is feasible on FFPE bone marrow trephine sections

Figure 1 demonstrates the performance of the individual primary antibody-fluorophore combinations on the exact same section of trephine tissue (Figure 1A-F) and illustrates a representative image (Figure 1G) of the merged 6-plex mIHC stain on a patient with myeloma.

Plasma cell percentage assessed by multiplex immunohistochemistry correlates to plasma cell percentage reported by diagnostic pathology

In clinical practice, the BMA PC percentage (%) is based on a manual, minimum 100 nucleated cell differential count, while the BMT PC burden is based on a visual estimation of anti-CD138 chromogenic IHC. Across the 156 samples assessed in this study, a matched-measures, one-way ANOVA demonstrated differences in the PC% reported by aspirate, CD138 IHC, and mIHC (*Online Supplementary Table S1*). On Dunn's multiple comparisons test, the difference was significant only between the aspirate and CD138 IHC, and the aspirate and mIHC groups (P<0.0001, respectively). There was no difference in PC burden as estimated by standard anti-CD138 IHC and mIHC in this study (P=0.9654). Spearman correlation coefficient between the aspirate

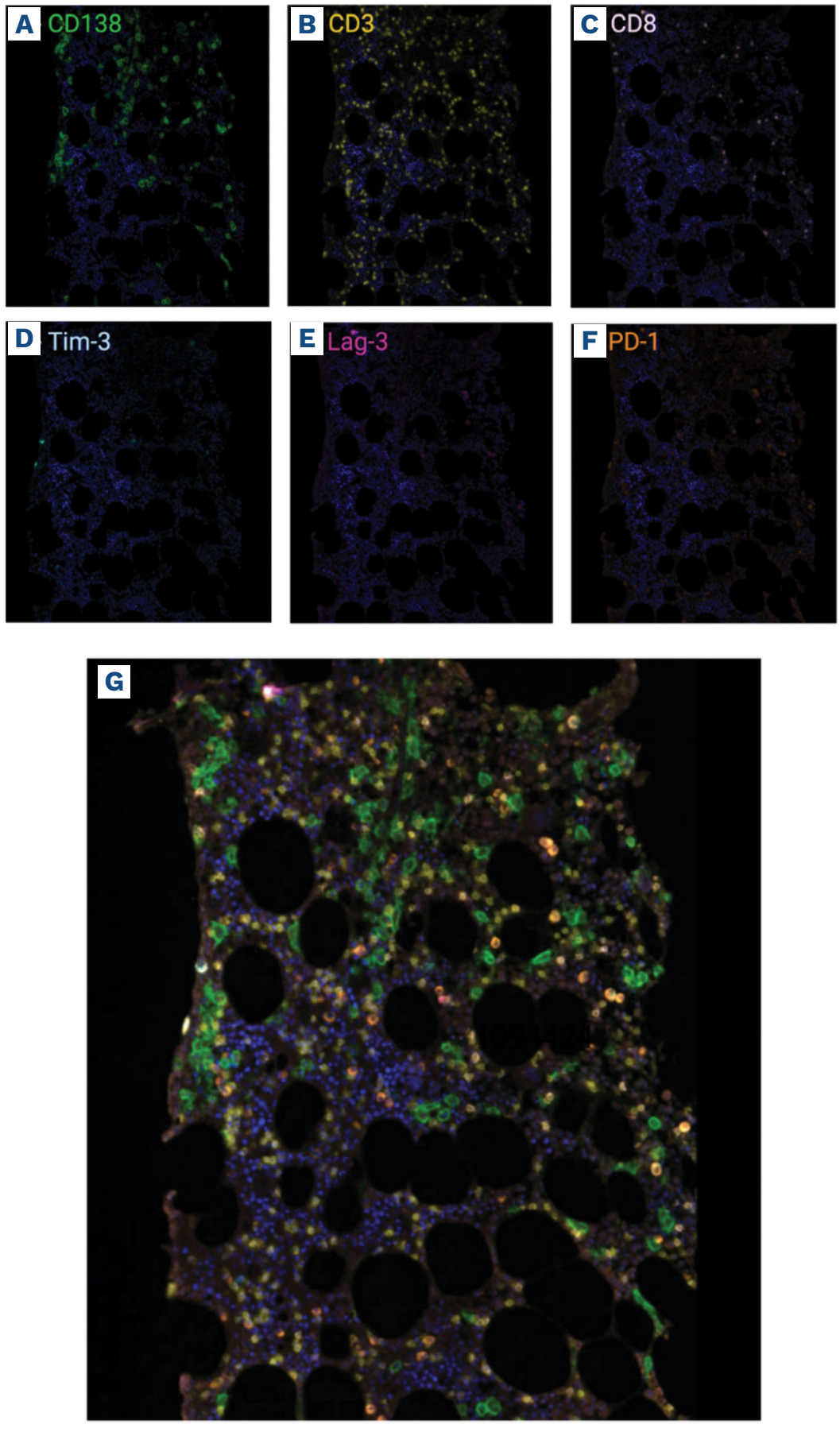

Figure 1. Multiplex immunohistochemistry. A formalin-fixed, paraffin-embedded section of bone marrow trephine was sequentially stained with primary antibody and immunofluorescent Opal™ fluorophore combinations. (A-F) CD138 = green; CD3 = yellow; CD8 = blush pink; Tim-3 = light blue; Lag-3 = pink, PD-1 = orange, followed by DAPI nuclear counterstain (dark blue) resulting in the merged 6-plex multiplex immunohistochemistry image shown in (G).

and CD138 measures was 0.83, 0.72 between aspirate and mIHC, and 0.79 between the two IHC-based techniques.

T cell to plasma cell ratio is highest in patients with monoclonal gammopathy of undetermined significance

Table 3 summarises findings from the mIHC analysis. There was no difference in BM cellularity, extent of fat space, or the total number of cells assessed per trephine across the three cohorts. As expected, the PC burden was higher in patients with NDMM (35.3±25.1%) and RRMM (30.1±26.2%) when compared to patients with MGUS (11.6±7.8%) (P<0.0001). There was a trend towards an increase in $CD3^+$ T cells in proportion to overall BM cellularity in patients with MGUS (13.9±9.5%) compared with NDMM (11.0±5.9%) or RRMM (11.1±7.7%) patients (P=0.08), with almost a third of all $CD3^+$ lymphocytes co-expressing CD8 in all three patient groups (Figure 2). There was no discernible difference in the overall prevalence of $CD3^+CD8^+$ cytotoxic T cells. The T-cell/PC and T_{cyt}/PC ratio was highest in patients with relapsed disease and MGUS, but there was no statistically significant difference when comparing these ratios in patients with ND and RR myeloma.

Lag-3$^+$ cytotoxic T cells are more prevalent than Tim-3 or PD-1$^+$ T cells within the bone marrow tumor microenvironment

The percentages of all nucleated cells within the BM trephine expressing the checkpoint receptors Tim-3, Lag-3, or PD-1 were similar between the three cohorts of patients, as was their co-expression on both CD3$^+$CD8$^+$ and CD3$^+$CD8$^-$ T cells (Figure 3). In ND patients, Tim3 was expressed on 3.45±5.31%, Lag3 on 6.18±6.17%, and PD-1 on 4.13±7.52% of cytotoxic CD3$^+$CD8$^+$ T cells and there was no significant difference in expression compared to relapsed patients. Of the three assessed checkpoint receptors, Lag3 was the most commonly found receptor on cytotoxic T cells in all patient groups (Table 4, Figure 3). PD-1, however, was the most common checkpoint receptor on CD8$^-$ T cells in patients with relapsed myeloma or MGUS.

Table 3. Summary of multiplex immunohistochemistry results.

Characteristics	MGUS N=32	NDMM N=65	RRMM N=59	*P*
BM cellularity, %	47.0±11.7	52.1±17.0	53.46±15.1	0.1984
Fat space, %	35.7±12.0	37.1±17.0	33.5±12.9	0.4050
Total N of nucleated cells assessed	31,549±20,270	39,723±27,853	33,537±26,472	0.4225
Plasma cells, %	11.6±7.8	35.3±25.1	30.1±26.2	<0.0001* 1 *vs.* 2 < 0.0001 1 *vs.* 3 = 0.0014 2 *vs.* 3 = 0.2511
Non-plasma cells, %	88.4±7.8	63.9±24.8	69.9±26.2	<0.0001* 1 *vs.* 2 < 0.0001 1 *vs.* 3 = 0.0014 2 *vs.* 3 = 0.2511
CD3 and CD8 expression, % CD3$^+$T cells (as % of all nucleated cells) CD3$^+$ CD8$^+$ T cells, (as % of all nucleated cells) Proportion of CD3$^+$ cells co-expressing CD8	 13.9±9.5 4.3±3.3 30.1±13.6	 11.0±5.9 3.5±3.0 33.3±19.3	 11.1±7.7 3.8±3.5 34.5±15.7	 0.0807 0.4679 0.4881
T-cell-to-plasma cell ratio				
CD3$^+$ T cell/PC ratio	1.97±2.24	0.73±1.19	1.65±3.95	<0.0001* 1 *vs.* 2 < 0.0001 1 *vs.* 3 < 0.0001 2 *vs.* 3 = 0.6846
CD3$^+$ CD8$^+$ T cell/PC ratio	0.65±0.93	0.23±0.44	0.66±1.82	<0.0001* 1 *vs.* 2 < 0.0001 1 *vs.* 3 = 0.0011 2 *vs.* 3 = 0.4565
Tim3 expression, % Tim3$^+$ cells Tim3$^+$ CD3$^+$ CD8$^+$ T cells Tim3$^+$ CD3$^+$ CD8$^-$ T cells % T_{cyt} expressing Tim3	 2.3±2.4 0.08±0.07 0.31±0.35 2.35±2.30	 3.4±4.2 0.13±0.25 0.56±0.89 3.45±5.31	 2.8±4.3 0.12±0.23 0.49±0.97 2.89±3.51	 0.4683 0.4895 0.7606 0.7439
Lag3 expression, % Lag3$^+$ cells Lag3$^+$ CD3$^+$ CD8$^+$ T cells Lag3$^+$ CD3$^+$ CD8$^-$ T cells % T_{cyt} expressing Lag3	 5.5±4.1 0.35±0.43 0.76±1.18 8.03±5.69	 6.1±7.7 0.25±0.38 0.83±1.44 6.18±6.17	 4.4±.59 0.27±0.35 0.53±0.83 7.79±8.81	 0.2367 0.1343 0.6276 0.1569
PD-1 expression, % PD-1$^+$ cells PD-1$^+$ CD3$^+$ CD8$^+$ T cells PD-1$^+$ CD3$^+$ CD8$^-$ T cells % T_{cyt} expressing PD1	 3.5±4.2 0.16±0.28 0.98±1.16 2.73±3.63	 5.4±8.2 0.15±0.30 0.92±1.45 4.13±7.52	 3.0±3.6 0.13±0.24 0.99±1.76 3.33±5.61	 0.5906 0.9355 0.2600 0.7846
Absolute number of CD3$^+$ CD8$^+$ T cells within a specified distance from PC Within 25 μm Within 50 μm Within 100 μm	 901.7±1,602 1,222±1,984 1,406±2,089	 1,215±1,989 1,379±2,093 1,464±2,163	 896.7±1,227 1,129±1,935 1,330±2,750	 0.3905 0.5139 0.4960

Continued on following page.

Characteristics	MGUS N=32	NDMM N=65	RRMM N=59	*P*
Proportion of $CD3^+$ $CD8^+$ T cells within a specified distance from PC, %				
Within 25 μm	54.7±21.2	79.3±22.0	68.2±28.8	<0.0001* 1 *vs.* 2 < 0.0001 1 *vs.* 3 = 0.0068 2 *vs.* 3 = 0.0860
Within 50 μm	77.6±19.5	90.8±15.8	81.5±23.9	<0.0001* 1 *vs.* 2 < 0.0001 1 *vs.* 3 = 0.0489 2 *vs.* 3 = 0.0385
Within 100 μm	92.8±12.7	96.9±9.2	92.3±16.8	0.0007* 1 *vs.* 2 = 0.0004 1 *vs.* 3 = 0.0342 2 *vs.* 3 = 0.406
Average distance to PC for each T_{cyt}, μm	38.1±28.3	23.5±32.1	30.0±27.6	<0.0001* 1 *vs.* 2 < 0.0001 1 *vs.* 3 = 0.0094 2 *vs.* 3 = 0.1305
Average number of T_{cyt} within 100 μm of a PC	1.77±0.65	1.60±1.27	1.62±1.33	0.0010 1 *vs.* 2 < 0.0018 1 *vs.* 3 = 0.0024 2 *vs.* 3 > 0.9999
Average distance to T_{cyt} for each PC, μm	50.9±27.1	76.6±67.5	97.7±219.3	0.2510
Proportion of unique plasma cells, %	25.6±15.8	11.5±11.5	15.0±17.5	<0.0001* 1 *vs.* 2 < 0.0001 1 *vs.* 3 = 0.0002 2 *vs.* 3 = 0.8437
Proportion of unique T_{cyt}, %	58.3±20.4	80.3±20.1	73.5±24.9	<0.0001* 1 *vs.* 2 < 0.0001 1 *vs.* 3 = 0.0023 2 *vs.* 3 = 0.3218

BM: bone marrow; MGUS: monoclonal gammopathy of undetermined significance; N: number; NDMM: newly diagnosed multiple myeloma; RRMM: relapsed and/or refractory multiple myeloma. Values represent mean ± Standard Deviation (SD). *Ordinary one-way ANOVA or Kruskal-Wallis tests as appropriate with corresponding Tukey's or Dunn's multiple comparisons tests where significance was detected between groups and where: 1 = MGUS, 2 = NDMM, and 3 = RRMM cohort.

Cytotoxic T cells are in closer proximity to plasma cells in patients with newly diagnosed disease

The percentage of cytotoxic T cells located within a 25 μm radius away from a PC was highest in patients with NDMM including smouldering myeloma (79.3±22%) when compared to patients with MGUS (54.7±21.2) or relapsed (68.2±28.8) disease (*P*<0.0001) (Figure 4C). This significant difference was maintained at both the 50 μm and 100 μm distance where almost 97% of cytotoxic T cells were within 100 μm of a PC in the trephine of ND patients. The average distance to a PC for each cytotoxic T cell was greater in patients with MGUS (38.1±28.3 μm) than patients with relapsed (30±27.6 μm; *P*=0.1305) or ND (23.5±32.1 μm) myeloma (*P*<0.0001). The average number of cytotoxic T cells within a 100 μm radius of a PC was highest in patients with MGUS (1.77±0.65 *vs.* 1.60±1.27 [ND] *vs.* 1.62±1.33 [RR]; *P*<0.001). The percentage of plasma cells with only a single cytotoxic T cell within a 100 μm radius was lowest in ND patients (11.5±11.5 *vs.* 25.6±15.8 [MGUS] *vs.* 16.5±20.6 [RR]; *P*<0.0001).

Poor response to first-line therapy is associated with higher plasma cell burden

To further explore the relationships between the tumor and the microenvironment, we stratified each cohort of patients and performed several sub-group analyses. (See *Online Supplementary Table S2* for a summary of the mIHC data from these subgroup analyses). In the MGUS cohort, a comparison of patients at low/intermediate risk of progression to myeloma (N=21) with those at intermediate-high/high risk of progression showed no discernible differences in the iTME components assessed. There was no difference in cytotoxic T-cell or checkpoint receptor expression between patients who had an objective response to first-line therapy (N=41) compared with those that progressed within 12 months or had a suboptimal response (<PR; N=18). Comparing the worst (<PR; N=12) with the best (>CR; N=9) responders, those responding poorly to first-line therapy had a higher PC% (40.0±21.7% *vs.* 19.0±14.5%; *P*=0.022), and a higher proportion of $CD3^+CD8^+$ T cells within 25 μm (88.7±10.2% *vs.* 64.7±17.9%; *P*=0.001), 50 μm, and 100 μm of

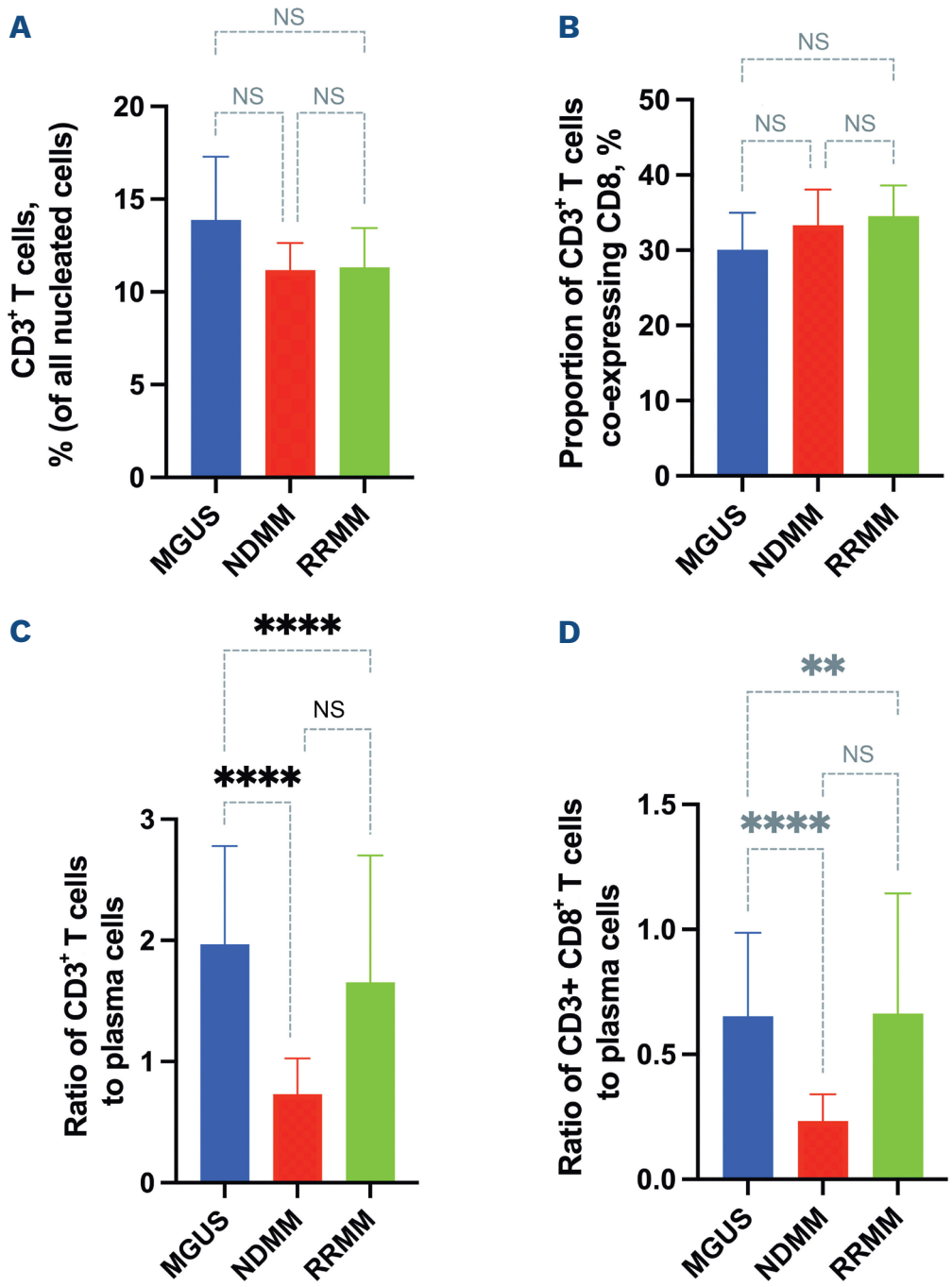

Figure 2. Increased CD3⁺ and CD3⁺CD8⁺ T cell to plasma cell ratio in patients with monoclonal gammopathy of undetermined significance. Multiplex immunohistochemistry demonstrates no difference in the proportion of CD3⁺ T cells or cytotoxic T cells between monoclonal gammopathy of undetermined significance (MGUS), and newly diagnosed (ND) and relapsed/refractory (RR) multiple myeloma (MM) patients (A and B), although the ratio of both CD3⁺ and cytotoxic T cells to plasma cells is highest in patients with MGUS (C and D). Values represent mean ±95% Confidence Interval. Pairwise comparisons: $^{**}P<0.01$, $^{****}P<0.0001$, ns: not significant.

a PC. Prior autoSCT was not associated with a difference in iTME, while less heavily pre-treated patients (1 prior line of therapy; N=22) had a higher proportion of cytotoxic T cells expressing Lag-3 than patients with >3 prior lines of therapy (N=14; 0.41±0.43% *vs.* 0.13±0.14%; P=0.025).

Discussion

Using mIHC, we are the first to report on the precise spatial distribution and relationship between immune cells and malignant PC within the BM of patients with MGUS, and ND and RR MM. Assessing a large cohort of trephine biopsies, we confirm previous reports that mIHC is a feasible and accurate application of quantitative pathology that can be used to assess the BM TME.[26]

In general, malignant PC tend to aggregate in small clusters or larger sheets of PC, occasionally overwhelming the BM. In the context of spatial heterogeneity being a hallmark of myeloma, and to avoid selection bias, we assessed the entire trephine available for each case. Each slide was assessed blinded with no discernible difference in the total BM area or number of cells assessed across the three cohorts. Estimation of the PC burden by mIHC is comparable to that reported by CD138 IHC used in standard diagnostic pathology and, in line with previous reports, PC quantification is consistently greater by either immunostaining method than by aspirate differential count.[27,28] Of interest, several patients in the MGUS cohort had an mIHC-derived PC% that would surpass the diagnostic criteria for myeloma, and while some patients diagnosed with MGUS may, indeed, have smouldering myeloma, when comparing the

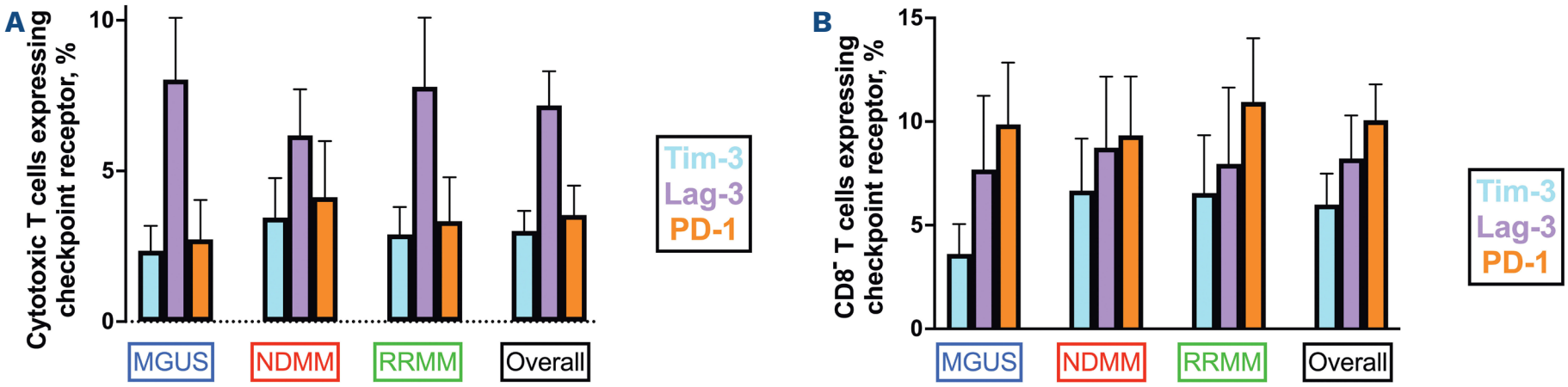

Figure 3. Checkpoint receptor expression on CD8⁺, cytotoxic T cells, and CD8⁻ T cells in patients with monoclonal gammopathy of undetermined significance, and newly diagnosed and relapsed/refractory multiple myeloma. Shown are the percentages of (A) cytotoxic T cells and (B) CD8⁻ T cells expressing the assessed checkpoint receptors Tim-3 (light blue), Lag-3 (blush pink), or PD-1 (orange) across the three cohorts of patients assessed. Values represent mean±95% Confidence Interval. MGUS: monoclonal gammopathy of undetermined significance; MM: multiple myeloma; ND: newly diagnosed; RR: relapsed/refractory.

PC% by trephine CD138 IHC and mIHC there was no difference between the two techniques (6.5±2.6% *vs.* 11.6±7.8%; *P*=0.313).[29] For the purpose of this study, and in keeping with guidelines according to which MM diagnosis is based on the BMA, no patients diagnosed with MGUS were reclassified to MM. We do, however, present a subgroup analysis of the MGUS cohort based on PC% (<10% *vs.* ≥10%) by mIHC (*Online Supplementary Table S3*). MGUS patients who by mIHC had ≥10% PC in the BMT, had a significantly higher number of CD3⁺ T cells, a trend towards higher CD3⁺CD8⁺ T cells, and increased Lag3⁺CD3⁺CD8⁺ T cells and significantly higher PD1⁺CD3⁺CD8⁻ T cells than MGUS patients with <10% PC by mIHC. The most intriguing finding was the higher number of T cells and Lag-3⁺ cytotoxic T cells, possibly indicative of an early immune response, and this should be further explored in future studies powered to address whether mIHC may predict the risk of progression to symptomatic myeloma.

With this multiplex panel, we set out to describe the dysregulated immune system by first assessing for quantitative changes in CD3⁺ and CD3⁺CD8⁺ cytotoxic T cells at various stages of the disease process and immune competency. The observed trend for a greater proportion of T cells expressing CD3 in the MGUS cohort may, in part, be representative of an anti-tumor response seen during the early stages of immune surveillance.[30] While our study did not show any difference in the proportion of cytotoxic T cells across MGUS, and ND and RR MM patients, we show that, in all three cohorts, approximately a third of all T cells co-express CD3 and CD8. BM infiltration with CD3⁺ T cells and CD8⁺ cytotoxic T cells as a fraction of the PC burden within the BM is significantly higher in patients with MGUS compared to ND and relapsed myeloma. While this may be due to a higher PC burden in the latter cohorts (which is consistent with previous reports of T-cell expansion in patients with MGUS), this finding is indicative of a relatively more pronounced immune landscape in this patient population.[31]

To assess for cytotoxic T-cell exhaustion, we examined the expression of three checkpoint receptors: Tim-3, Lag-3, and PD-1. In addition to suppressing cytotoxic T-cell function, these checkpoints are present on, and modulate the function of, CD4⁺ helper T cells, regulatory T cells, and natural killer cells, among others.[32-34] Comprehensive molecular and phenotypic profiling of peripheral blood T cells isolated from patients with myeloma following an autoSCT not only demonstrates persistent checkpoint expression, but recognizes Lag-3 and PD-1 as potential immune biomarkers for identifying patients at higher risk of relapse.[9,35] Comparing the three cohorts of patients, we found no difference in the proportion of nucleated cells expressing Tim-3, Lag-3, or PD-1 on their cell surface, nor their prevalence on CD8⁺ or CD8⁻ T cells. The similar expression pattern in both the ND and RR cohort indicates the potential of checkpoint receptor inhibition in both the treatment naïve and the relapsed setting. Lag-3 was more prominent on cytotoxic T cells, suggesting Lag-3 inhibition may be effective in MM and may have synergistic potential with PD-1, which is over-expressed on CD8⁻ T cells. However, interestingly, Lag3 was consistently the most prevalent checkpoint receptor on cytotoxic T cells of patients with MGUS, and ND and RR myeloma while PD-1 is more pronounced on CD8⁻ T cells. In addition, within the relapsed cohort of patients, those with fewer prior lines of therapy had a higher proportion of cytotoxic T cells expressing Lag-3 compared with the heavily pre-treated patients. Thus, our data suggest that early therapeutic modulation of Lag-3 may be associated with more pronounced augmentation and restoration of cytotoxic T-cell function than may be achieved with anti-Tim-3 or anti-PD-1 blockade alone or if delivered after several lines of therapy. Targeting of Lag-3 may also provide the added benefit of dampening the immunosuppressive effect of Lag-3 expressing regulatory T cells.[32] A recent study examining the pre- and post-transplant, transcriptional profile of peripheral blood T cells demonstrated an increase in Lag-3, specifically in the CD4⁺ T-cell subset,

Table 4. Tim-3, Lag-3, and PD-1 expression by multiplex immunohistochemistry.

	Tim3	Lag3	PD-1	*P*
Checkpoint receptor expression, % of all nucleated cells				
MGUS, N=32	2.3±2.4	5.5±4.1	3.5±4.2	0.0024* 1 *vs.* 2 = 0.0053 1 *vs.* 3 > 0.9999 2 *vs.* 3 = 0.0121
NDMM, N=65	3.6±4.5	6.1±7.7	5.4±8.2	0.3432
RRMM, N=59	3.2±5.3	4.3±6.0	3.3±4.5	0.0687
Combined, N=156	3.2±4.5	5.4±6.5	4.2±6.3	0.0024* 1 *vs.* 2 = 0.0023 1 *vs.* 3 > 0.9999 2 *vs.* 3 = 0.0484
Proportion of cytotoxic T cells expressing checkpoint receptor of interest, %				
MGUS, N=32	2.4±2.3	8.0±5.7	2.7±3.6	<0.0001 1 *vs.* 2 = 0.0003 1 *vs.* 3 = 0.7270 2 *vs.* 3 < 0.0001
NDMM, N=65	3.5±5.3	6.2±6.2	4.1±7.5	0.0048 1 *vs.* 2 = 0.0130 1 *vs.* 3 > 0.9999 2 *vs.* 3 = 0.0149
RRMM, N=59	2.9±3.5	7.8±8.8	3.3±5.6	<0.0001 1 *vs.* 2 = 0.0025 1 *vs.* 3 >0.9999 2 *vs.* 3 = 0.0001
Combined, N=156	3.0±4.2	7.2±7.2	3.5±6.2	<0.0001 1 *vs.* 2 < 0.0001 1 *vs.* 3 > 0.9999 2 *vs.* 3 < 0.0001
Proportion of CD8$^-$ lymphocytes expressing checkpoint receptor of interest, %				
MGUS, N=32	3.6±4.0	7.7±9.9	9.9±8.3	0.0059 1 *vs.* 2 > 0.9999 1 *vs.* 3= 0.0058 2 *vs.* 3 = 0.0720
NDMM, N=65	6.7±10.0	8.7±13.6	9.3±11.3	0.1740
RRMM, N=59	6.5±10.7	8.0±14.1	7.9±14.0	0.0292 1 *vs.* 2 > 0.9999 1 *vs.* 3= 0.0626 2 *vs.* 3 = 0.0656
Combined, N=156	6.0±9.4	8.2±13.1	10.1±10.9	<0.0001 1 *vs.* 2 > 0.9999 1 *vs.* 3= 0.0001 2 *vs.* 3 = 0.0027

MGUS: monoclonal gammopathy of undetermined significance; N: number; NDMM: newly diagnosed multiple myeloma; RRMM: relapsed and/or refractory multiple myeloma. Values represent % of bone marrow cells identified; mean ± Standard Deviation (SD). *Kurskal-Wallis one-way ANOVA for non-parametric data with corresponding Dunn's multiple comparisons tests shown where: 1 = Tim-3, 2 = Lag-3, and 3 = PD-1 expression.

and adverse outcomes.[9] Therapeutic targeting of Lag-3 has been shown to enhance T-cell proliferation and their anti-myeloma activity.[14] Indeed, monoclonal antibodies against all three checkpoint receptors are at diverse stages of pre-clinical and clinical development, with some studies even assessing combination therapy aimed at overcoming the upregulation of non-targeted checkpoints as a means of a potential mechanism of resistance.[34,36-38]

While many have published and reviewed on the quantitative and qualitative changes observed within the T-cell repertoire of patients with PC dyscrasias, using mIHC, our study is unique in allowing us to comment on the spatial relationships between the tumor and the immune cells.[5,6,22,39-41] At 5 μm intervals, we examined the distribution of cytotoxic T cells within a 100 μm radius of each PC. The difference in the absolute number of cytotoxic

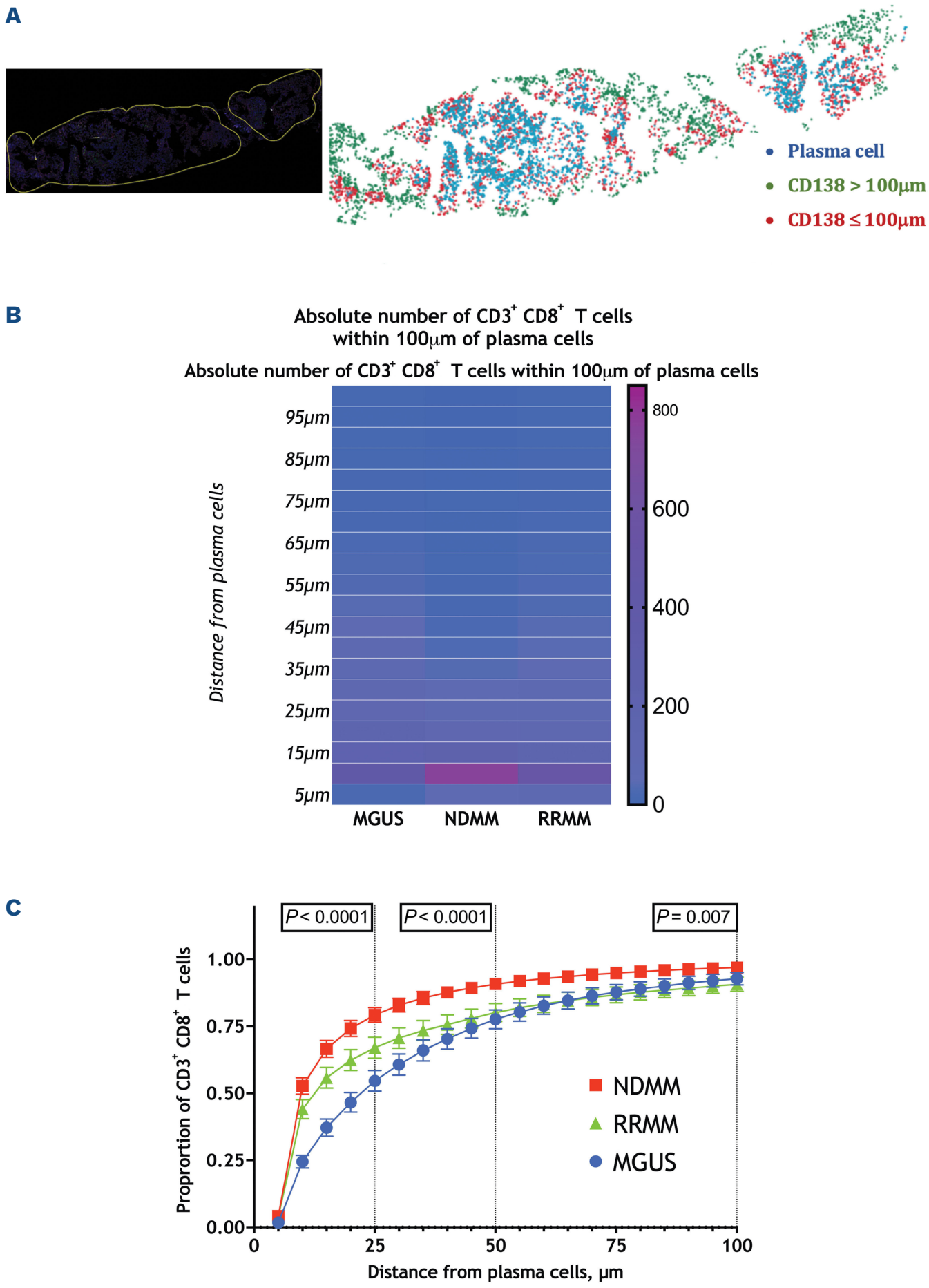

Figure 4. Nearest neighbor and proximity analysis. (A) Whole slide scan overview of bone marrow trephine and Halo™ spatial analysis plot illustrating plasma cells (blue), cytotoxic T cells within 100 µm (red) and greater than 100 µm (green) away from a plasma cell. Cytotoxic T-cell heat map demonstrating (B) the absolute number and (C) the proportion of cytotoxic T cells at 5 µm intervals within a 100 µm radius of plasma cells in the three patient groups. MGUS: monoclonal gammopathy of undetermined significance; MM: multiple myeloma; ND: newly diagnosed; RR: relapsed/refractory.

T cells in proximity to PC was similar between the three cohorts, although the proportion of all cytotoxic T cells within the 25 µm, 50 µm, and 100 µm radius was higher in ND than in relapsed patients, while a still smaller fraction was in proximity to PC in patients with MGUS. While this may be secondary to higher PC burden in myeloma, both NDMM and RRMM patients have a higher PC% than MGUS patients (11.6±7.8%) with no difference between NDMM and RRMM patients (35.3±25.1% *vs.* 30.1±26.2; *P*=0.2511). Nevertheless, the proportion of cytotoxic T cells within

50 μm in the NDMM and RRMM cohorts differed (90.8±15.8 *vs.* 81.5±23.9; *P*=0.0385), suggesting that PC burden is not the main determinant of the plasma cell/cytotoxic T-cell spatial relationship.

We assessed the spatial relationship between plasma cells and cytotoxic T cells in a bi-directional manner. The average distance from each PC to a cytotoxic T cell is more dependent on the degree and pattern of PC infiltration, while the T cell to PC relationship is more dependent on active migration of cytotoxic T cells and a function of the immune system. The average distance from each PC to a cytotoxic T cell in ND patients was 76.6 μm, reflective of the propensity of PC to aggregate in clusters within the BM. In one ND patient, the average distance from each cytotoxic T cell to a PC was 23.5 μm, which is just greater than the average size of a PC (14-20 μm).[42] The average distance between cytotoxic T cells and PC increased to 30.0 μm in relapsed patients, and was significantly greater in patients with MGUS (38.1 μm), suggesting more active migration of cytotoxic T cells towards PC. In addition, ND patients had the lowest percentage of unique PC (i.e., PC with only a single cytotoxic T cell within a 100 μm radius), and conversely, the highest number of unique cytotoxic T cells. Together these findings suggest that the proximity of cytotoxic T cells to PC in ND patients may be reflective of a more robust immune response during the early stages of the disease process as opposed to later stages of myeloma. Others have demonstrated that the response to checkpoint-directed immunotherapy in patients with metastatic melanoma may be predicted by the density and proximity of immune cells to melanoma cells.[19] In our cohort of newly diagnosed patients, comparing those achieving complete response or, even better, with those failing to achieve at least a partial response, the percentage of all cytotoxic T cells with proximity to PC was significantly greater in patients failing to respond. The myeloma treatment landscape is rapidly evolving, with a steady input of immune-based therapies, and it remains imperative to enhance our understanding of the spatial relationship between cytotoxic T cells and PC at various stages of the disease process in order to better understand what may predict response to these new therapeutics. Our study identifies mIHC as a feasible method, and future studies should serially track the iTME composition and spatial relationships in a cohort of uniformly treated patients at baseline, after a pre-defined period of treatment, and at the time of disease progression.

The major drawback of mIHC is the inherent limitation to six markers within a single panel, which does not allow a more detailed exploration of the intricate relationships between the tumor and the microenvironment. Analysis of consecutive FFPE sections with additional panels would partially overcome this shortcoming; however, emerging reports on the use of high-throughput imaging mass cytometry assessing up to 40 markers while also preserving spatial architecture are promising.[43,44] While we examined a large cohort of patients, we ensured that all samples assessed were from the same institution, having undergone the exact same fixation and decalcification process. Nevertheless, there is considerable variation in the age of sections, which may introduce variability in staining performance and tissue integrity. The marked heterogeneity of treatment regimens in both the upfront and relapsed setting makes identification of biomarkers of response to therapy difficult, and interpretation of some of the pre-specified subgroup analyses were limited by the small sample size. Importantly, mIHC does not provide information concerning the functional status of the iTME and we did not assess whether the pattern of BM infiltration (diffuse *vs.* nodular) is a potential biomarker that may impact the ability of T cells to access PC.

In conclusion, our study is the first to report on the spatial relationship of cytotoxic $CD8^+$ T cells and PC using mIHC on FFPE BM trephine sections from patients with PC dyscrasias. The demonstrated proximity of cytotoxic T cells to malignant PC during the early stages of MM should be further explored as a potential biomarker of response to T-cell engagers, with the hypothesis that closer proximity may translate to improved efficacy. We also show a higher proportion of cytotoxic T cells expressing Lag-3 in patients with early, as opposed to late, relapsed myeloma. This supports the need for further investigation of Lag-3 inhibition in myeloma, possibly in combination with PD-1 inhibition, given its overexpression on $CD8^-$ T cells. Future studies should examine additional markers (including other checkpoint receptors) and the impact on other immune T-cell subsets and on serial sections. Ideally, such studies should track changes in the microenvironment in individual patients after treatment, with the aim of identifying robust biomarkers of response and resistance, and to facilitate sequencing of therapies in an ever-growing therapeutic landscape.

Disclosures

SJH reports consulting or advisory roles for Celgene, Hoffman-La Roche AG, Genetech USA, HaemaLogiX, Janssen Global Services, Novartis, and research support from HaemaLogiX and Janssen Global Services. HQ reports consulting or advisory roles for Amgen, Antegene, Bristol-Myers Squibb/Celgene, Celgene, GSK, Janssen-Cilag, Karyopharm Therapeutics, Pfizer, Roche, and Sanofi, and research support from Amgen, Bristol-Myers Squibb/Celgene, Celgene, GSK, Karyopharm Therapeutics, and Sanofi. SN and LEP have no conflicts of interest to disclose.

Contributions

All authors designed the study. SN applied for research governance approval, identified eligible patients, collated retrospective clinical data, reviewed, and analyzed multiplex images, correlated image and clinical data, performed

statistical analyses, prepared figures and tables, and wrote the initial draft manuscript. LEP, SJH and HQ supervised the study and critically reviewed the manuscript. All authors reviewed and approved the final version for publication.

Acknowledgments

The authors would like to acknowledge the expertise and assistance of Dr. Rejhan Idrizi from the Centre for Advanced Histology & Microscopy (CAHM), Peter MacCallum Cancer Centre, Victoria, Australia.

Funding

This work was supported by the Australian Government Research Training and Program Scholarship (to SN) and a Victorian Cancer Agency Grant (to HQ).

Data-sharing statement

Original data and protocol(s) may be obtained upon written request.

References

1. Cohen AD. Myeloma: next generation immunotherapy. Hematology. 2019;2019(1):266-272.
2. Ninkovic S, Quach H. Shaping the treatment paradigm based on the current understanding of the pathobiology of multiple myeloma: an overview. Cancers. Cancers (Basel). 2020;12(11):3488.
3. Soekojo CY, Ooi M, De Mel S, Chng WJ. Immunotherapy in multiple myeloma. Cells. 2020;9(3):601.
4. Dosani T, Carlsten M, Maric I, Landgren O. The cellular immune system in myelomagenesis: NK cells and T cells in the development of myeloma and their uses in immunotherapies. Blood Cancer J. 2015;5(7):e306.
5. Raitakari M, Brown RD, Sze D, et al. T-cell expansions in patients with multiple myeloma have a phenotype of cytotoxic T cells. Br J Haematol. 2000;110(1):203-209.
6. Pessoa De Magalhaes RJ, Vidriales M-B, Paiva B, et al. Analysis of the immune system of multiple myeloma patients achieving long-term disease control by multidimensional flow cytometry. Haematologica. 2013;98(1):79-86.
7. Zelle-Rieser C, Thangavadivel S, Biedermann R, et al. T cells in multiple myeloma display features of exhaustion and senescence at the tumor site. J Hematol Oncol. 2016;9(1):e321.
8. Tan J, Chen S, Huang J, et al. Increased exhausted CD8(+) T cells with programmed death-1, T-cell immunoglobulin and mucin-domain-containing-3 phenotype in patients with multiple myeloma. Asia Pac J Clin Oncol. 2018;14(5):e266-e274.
9. Lucas F, Pennell M, Huang Y, et al. T cell transcriptional profiling and immunophenotyping uncover LAG3 as a potential significant target of immune modulation in multiple myeloma. Biol Blood Marrow Transplant. 2020;26(1):7-15.
10. Kwon M, Kim CG, Lee H, et al. PD-1 Blockade reinvigorates bone marrow CD8(+) T cells from patients with multiple myeloma in the presence of TGFβ inhibitors. Clin Cancer Res. 2020;26(7):1644-1655.
11. Guillerey C, Harjunpää H, Carrié N, et al. TIGIT immune checkpoint blockade restores CD8(+) T-cell immunity against multiple myeloma. Blood. 2018;132(16):1689-1694.
12. Batorov EV, Aristova TA, Sergeevicheva VV, et al. Quantitative and functional characteristics of circulating and bone marrow PD-1- and TIM-3-positive T cells in treated multiple myeloma patients. Sci Rep. 2020;10(1):20846.
13. Kreiniz N, Eiza N, Tadmor T, et al. The involvement of LAG3+ plasma cells in the development of multiple myeloma. Blood. 2022;140(Suppl 1):7112-7113.
14. Bae J, Accardi F, Hideshima T, et al. Targeting LAG3/GAL-3 to overcome immunosuppression and enhance anti-tumor immune responses in multiple myeloma. Leukemia. 2022;36(1):138-154.
15. Minnie SA, Kuns RD, Gartlan KH, et al. Myeloma escape after stem cell transplantation is a consequence of T-cell exhaustion and is prevented by TIGIT blockade. Blood. 2018;132(16):1675-1688.
16. Mateos MV, Orlowski RZ, Ocio EM, et al. Pembrolizumab combined with lenalidomide and low-dose dexamethasone for relapsed or refractory multiple myeloma: phase I KEYNOTE-023 study. Br J Haematol. 2019;186(5):e117-e121.
17. Badros A, Hyjek E, Ma N, et al. Pembrolizumab, pomalidomide, and low-dose dexamethasone for relapsed/refractory multiple myeloma. Blood. 2017;130(10):1189-1197.
18. Mateos M-V, Blacklock H, Schjesvold F, et al. Pembrolizumab plus pomalidomide and dexamethasone for patients with relapsed or refractory multiple myeloma (KEYNOTE-183): a randomised, open-label, phase 3 trial. Lancet Haematol. 2019;6(9):e459-e469.
19. Gide TN, Silva IP, Quek C, et al. Close proximity of immune and tumor cells underlies response to anti-PD-1 based therapies in metastatic melanoma patients. OncoImmunology. 2020;9(1):1659093.
20. Li F, Li C, Cai X, et al. The association between CD8+ tumor-infiltrating lymphocytes and the clinical outcome of cancer immunotherapy: a systematic review and meta-analysis. EClinicalMedicine. 2021;41:101134.
21. Fu T, Dai L-J, Wu S-Y, et al. Spatial architecture of the immune microenvironment orchestrates tumor immunity and therapeutic response. J Hematol Oncol. 2021;14(1):98.
22. Zavidij O, Haradhvala NJ, Mouhieddine TH, et al. Single-cell RNA sequencing reveals compromised immune microenvironment in precursor stages of multiple myeloma. Nat Cancer. 2020;1(5):493-506.
23. Wang J, Hu Y, Hamidi H, et al. Immune microenvironment characteristics in multiple myeloma progression from transcriptome profiling. Front Oncol. 2022;12:948548.
24. Dhodapkar KM, Cohen AD, Kaushal A, et al. Changes in bone marrow tumor and immune cells correlate with durability of remissions following BCMA CAR T therapy in myeloma. Blood Cancer Discov. 2022;3(6):490-501.
25. Bird J, Behrens J, Westin J, et al. UK Myeloma Forum (UKMF) and Nordic Myeloma Study Group (NMSG): guidelines for the investigation of newly detected M-proteins and the management of monoclonal gammopathy of undetermined significance (MGUS). Br J Haematol. 2009;147(1):22-42.
26. Walters DK, Jelinek DF. Multiplex immunofluorescence of bone

marrow core biopsies: visualizing the bone marrow immune contexture. J Histochem Cytochem. 2020;68(2):99-112.
27. Ng AP, Wei A, Bhurani D, Chapple P, Feleppa F, Juneja S. The sensitivity of CD138 immunostaining of bone marrow trephine specimens for quantifying marrow involvement in MGUS and myeloma, including samples with a low percentage of plasma cells. Haematologica. 2006;91(7):972-975.
28. Joshi R, Horncastle D, Elderfield K, Lampert I, Rahemtulla A, Naresh KN. Bone marrow trephine combined with immunohistochemistry is superior to bone marrow aspirate in follow-up of myeloma patients. J Clin Pathol. 2008;61(2):213-216.
29. Rajkumar SV, Dimopoulos MA, Palumbo A, et al. International Myeloma Working Group updated criteria for the diagnosis of multiple myeloma. Lancet Oncol. 2014;15(12):e538-e548.
30. Mittal D, Gubin MM, Schreiber RD, Smyth MJ. New insights into cancer immunoediting and its three component phases-elimination, equilibrium and escape. Curr Opin Immunol. 2014;27:16-25.
31. Pérez-Andres M, Almeida J, Martin-Ayuso M, et al. Characterization of bone marrow T cells in monoclonal gammopathy of undetermined significance, multiple myeloma, and plasma cell leukemia demonstrates increased infiltration by cytotoxic/Th1 T cells demonstrating a squed TCR-Vβ repertoire. Cancer. 2006;106(6):1296-1305.
32. Camisaschi C, Casati C, Rini F, et al. LAG-3 expression defines a subset of CD4(+)CD25(high)Foxp3(+) regulatory T cells that are expanded at tumor sites. J Immunol. 2010;184(11):6545-6551.
33. Ruffo E, Wu RC, Bruno TC, Workman CJ, Vignali DAA. Lymphocyte-activation gene 3 (LAG3): the next immune checkpoint receptor. Semin Immunol. 2019;42:101305.
34. Wolf Y, Anderson AC, Kuchroo VK. TIM3 comes of age as an inhibitory receptor. Nat Rev Immunol. 2020;20(3):173-185.
35. Chung DJ, Pronschinske KB, Shyer JA, et al. T-cell exhaustion in multiple myeloma relapse after autotransplant: optimal timing of immunotherapy. Cancer Immunol Res. 2016;4(1):61-71.
36. Andrews LP, Marciscano AE, Drake CG, Vignali DAA. LAG3 (CD223) as a cancer immunotherapy target. Immunol Rev. 2017;276(1):80-96.
37. Salik B, Smyth MJ, Nakamura K. Targeting immune checkpoints in hematological malignancies. J Hematol Oncol. 2020;13(1):111.
38. Tawbi HA, Schadendorf D, Lipson EJ, et al. Relatlimab and nivolumab versus nivolumab in untreated advanced melanoma. N Engl J Med. 2022;386(1):24-34.
39. Bryant C, Suen H, Brown R, et al. Long-term survival in multiple myeloma is associated with a distinct immunological profile, which includes proliferative cytotoxic T-cell clones and a favourable Treg/Th17 balance. Blood Cancer J. 2013;3(9):e148.
40. Favaloro J, Brown R, Aklilu E, et al. Myeloma skews regulatory T and pro-inflammatory T helper 17 cell balance in favor of a suppressive state. Leuk Lymphoma. 2014;55(5):1090-1098.
41. Dhodapkar MV, Krasovsky J, Osman K, Geller MD. Vigorous premalignancy-specific effector T cell response in the bone marrow of patients with monoclonal gammopathy. J Exp Med. 2003;198(11):1753-1757.
42. Allen HC, Sharma P. Histology, Plasma Cells. In: StatPearls. [Internet]: Treasure Island (FL); StatPearls Publishing. https://www.ncbi.nlm.nih.gov/books/NBK556082/ Accessed January 24, 2022.
43. Ijsselsteijn ME, van der Breggen R, Farina Sarasqueta A, Koning F, de Miranda NFCC. A 40-marker panel for high dimensional characterization of cancer immune microenvironments by imaging mass cytometry. Front Immunol. 2019;10:2534.
44. Le Rochais M, Hemon P, Pers JO, Uguen A. Application of high-throughput imaging mass cytometry hyperion in cancer research. Front Immunol. 2022;13:859414.